

General Disclaimer

One or more of the Following Statements may affect this Document

- This document has been reproduced from the best copy furnished by the organizational source. It is being released in the interest of making available as much information as possible.
- This document may contain data, which exceeds the sheet parameters. It was furnished in this condition by the organizational source and is the best copy available.
- This document may contain tone-on-tone or color graphs, charts and/or pictures, which have been reproduced in black and white.
- This document is paginated as submitted by the original source.
- Portions of this document are not fully legible due to the historical nature of some of the material. However, it is the best reproduction available from the original submission.

NASA TECHNICAL
MEMORANDUM

NASA TM X-67857

NASA TM X-67857

NUCLEAR DESIGN AND EXPERIMENTS FOR A
SPACE POWER REACTOR

by Wendell Mayo, Paul G. Klann,
and Charles L. Whitmarsh, Jr.

Lewis Research Center
Cleveland, Ohio

TECHNICAL PAPER proposed for presentation at
American Nuclear Society Meeting
Boston, Massachusetts, June 13-17, 1971

FACILITY FORM 602

N 71 - 28820
(ACCESSION NUMBER)
21
(PAGES)
TMX-67857
(NASA CR OR TMX OR AD NUMBER)

(THRU)
G3
(CODE)
22
(CATEGORY)



NUCLEAR DESIGN AND EXPERIMENTS FOR A SPACE POWER REACTOR

by Wendell Mayo, Paul G. Klann, and Charles L. Whitmarsh, Jr.
Lewis Research Center

INTRODUCTION

The Lewis Research Center is conducting a technology program in support of a compact fast spectrum reactor to be used as a heat source for generating electric power in space. To provide a focal point, a reference reactor has been chosen and performance goals established. The reactor is to operate at a thermal power level of 2 megawatts for 50 000 hours with a lithium 7 coolant outlet temperature of 1222 K and would provide about 500 kilowatts of electric power from a Brayton cycle power conversion system.

The reasons for selecting this reference reactor and details of the mechanical design, thermal and hydraulic aspects, fuel swelling, and reactor dynamics are discussed in reference 1. Reference 2 discusses materials compatibility and irradiation experiments for this reactor.

It is the purpose of this report to summarize and describe the nuclear design characteristics of the reference reactor, to present results of critical experiments which have been conducted by Atomics International to check nuclear calculations, and to discuss alternate reactor designs which have been considered.

REFERENCE REACTOR

Description of the Reference Reactor

Figure 1 shows an isometric and figure 2 shows a cross section of the reference reactor. The core consists of 181 fuel elements arranged in the shape of a six-pointed star and located by a honeycomb core support structure. Reactivity control is achieved by six rotating fuel drums containing 11 fuel elements each. The control drums are imbedded in a TZM (a molybdenum alloy) radial reflector and located between the points of the star. A 0.635-centimeter thick T-111 (a tantalum alloy) pressure vessel encloses the reactor. The 5.06-centimeter thick end reflectors (TZM) are separated from the active core by grid plates, into which the fuel elements are anchored, and by coolant plenums which distribute lithium 7 coolant to the single pass flow channels.

The fuel elements fit within the honeycomb core support structure consisting of 2.16-centimeter diameter (0.025-cm thick) tubes welded along points of contact. This honeycomb structure provides uniform annular coolant flow passages (0.102-cm thick) for each fuel element and also provides a means of limiting fuel element bowing. Also indicated on figure 2 are the three zones of fuel volume fractions used to

flatten the radial power distribution. The fuel volume fractions in the unit cells (defined for calculation purposes) indicated on the figure are chosen to satisfy fuel burnup criteria so as to limit diametral creep in the fuel pin cladding to less than 1 percent over the 50 000 hour core life (discussed in more detail later). An additional important benefit of fuel zoning is enhanced reactivity worth of the control drums.

Figure 3 shows a cross section of a unit fuel cell. The uranium nitride (93.2 percent uranium 235) volume fraction is varied by varying the central hole (void) diameter. The void provides space for the accumulation of released fission product gases and for some fuel swelling, although the majority of the fuel swelling is in the axial direction. Crushable spacers (vibration suppressors) are provided at the ends of the fuel pin to accommodate axial deformation. Active fuel length is 37.6 centimeters. The tungsten liner (0.013-cm thick) acts as a separator to prevent physical contact between the UN fuel and the T-111 clad (0.147-cm thick).

Total coolant mass flow is 9.4 kilograms per second. Eighty four percent of the lithium 7 coolant flows in the 0.102-centimeter thick annulus between the clad and the honeycomb tube. Most of the remainder flows around the control drums, in the reflector and in the triflute spaces between adjacent honeycomb tubes. The flow rate in the triflute spaces is orificed to a low value. Additional details on the reference reactor heat transfer can be found in references 1 and 3.

Analysis and Results

Methods. - Multigroup cross sections used were generated by the GAM-II program (ref. 4). The GAM-II cross section library was used inasmuch as reevaluated ENDF/B cross sections were not available. Two basic energy group structures were routinely employed; a 13 fast energy group set ($E > 0.414$ eV) has been used for one dimensional calculations with the TDSN program (ref. 5), which is a one- or two-dimensional discrete ordinates transport program, and a four energy group set (a condensation of the 13 group set) is used for two dimensional (RZ or XY) calculations with the TDSN program and also for R θ calculations with the DOT-IIW transport program (ref. 6). When a thermal group is required, e.g., a water immersion accident, the GATHER-II program (ref. 7) is used to obtain thermal cross sections.

Figure 4 shows a typical XY model for the reference reactor with the control drums in the fuel fully inserted position. The XY grid used is shown superimposed on the actual geometry. Transverse leakage is accounted for by first performing an RZ calculation to incorporate the axial end reflectors and then establishing an effective core height for use in computing axial buckling terms for use in the XY (or R θ) model. The symmetry of the 1/4 core geometry is useful for most calcu-

lations; but with the requirement that all drums rotate in the same direction, it is necessary to use 1/2 core geometry to calculate the case of two adjacent control drums stuck in their most reactive positions. The DOT-IIW $R\theta$ model is most convenient for all drums partially rotated and was used in obtaining the radial power distribution and reactivity control as a function of time.

Power distributions. - As the control drums rotate from their start-up hot critical position of 118° to fuel full-in position of 180° at the end of core life, the radial power distribution changes with the fuel movement. On the other hand, the axial power distribution remains fairly constant with a maximum-to-average power ratio of \hat{P}_z/\bar{P}_z of 1.23. Figure 5 shows the result of time-averaging the local radial power distribution (P_r/\bar{P}_r) over 50 000 hours of core life. The fuel pins with the highest P_r/\bar{P}_r for each fuel zone are noted on the figure by A, B, C, and D.

In this type of reactor, which is fuel clad material creep limited, it is desirable to zone the power so as to equalize clad stress in each fuel pin. This is illustrated by figure 6 in which the curve shows the allowable value of P_r/\bar{P}_r as a function of volume fraction of fuel in a cell which will limit clad creep to one percent in 50 000 hours. The curve was derived from a fuel swelling analysis as described in references 1 and 3.

The fuel pins with the highest P_r/\bar{P}_r noted on figure 5 are also shown on figure 6 along with the range of variation as the control drums are rotated. Note that a fuel drum pin is closest to the limit curve.

Reactivity and reactivity control requirements. - The calculated available control swing (drums: fuel full-out to fuel full-in) is 8.51 percent $\Delta k/k$. Table 1 shows how the control swing is used. Fuel burnup (U^{235} atoms destroyed) requires 1.47 percent $\Delta k/k$ over 50 000 hours. The temperature defect, which includes 0.26 percent $\Delta k/k$ for coolant expansion, 0.58 percent $\Delta k/k$ for fuel and structure expansion and 0.25 percent $\Delta k/k$ for Doppler effect, requires a total of 1.09 percent $\Delta k/k$. The coolant temperature operating range is from 460 K, the melting point of the coolant, to 1222 K, the coolant outlet temperature. Long term axial fuel swelling requires 0.95 percent $\Delta k/k$. With an uncertainty allowance of 0.61 percent $\Delta k/k$, the total excess reactivity required is 4.12 percent $\Delta k/k$. The further required ability to shut down to a k_{eff} of 0.99 with any two of the six control drums stuck in their most reactive position requires an additional shutdown margin of 4.39 percent $\Delta k/k$; this includes 0.54 percent $\Delta k/k$ for drum interactions for the case of two adjacent stuck drums.

Additional details. - The total flux at rated power is about 1.02×10^{14} neutrons per square centimeter per second; about one-third of this flux are for neutrons of energies greater than 0.8 MeV. The median flux energy is 0.44 MeV and the median fission energy is

0.36 MeV.

The prompt neutron lifetime is calculated as 40 nanoseconds and the effective delayed neutron fraction is calculated as 0.0067 based on a delayed neutron fractional yield of 0.0065.

A partial "water immersion accident" simulated by surrounding the pressure vessel of the reactor radially by water increases the reactivity by 0.49 percent $\Delta k/k$. A total loss of coolant is equivalent to -1.52 percent $\Delta k/k$.

CRITICAL EXPERIMENTS

A series of critical experiments was performed by Atomics International (contract NAS-12982) to provide checks on the neutronic calculational methods and cross sections used for the reference reactor and to provide experimental information on reactivity effects and control drum worths. Reference 8 gives complete details of all experiments; representative experiments and comparisons with calculations are presented here.

Description of the Critical Assembly

Figure 7 is a photograph of the critical assembly. It was designed to provide a good geometric representation of the reference reactor. Figure 8 is a cross section of the critical assembly which shows the degree of similarity attained when compared with figure 2 showing the reference reactor. Fine control is obtained by rotating control drums as for the reference reactor. A scram device for the assembly relies on rapidly tilting two-thirds of the radial reflector away from the core. Provision is also made for the reactivity measurement of samples of materials of interest at the positions marked "S" on the figure. The samples are about 1.3 centimeters in diameter and extend the full length of the active core. The reactivity measurements are made relative to void using the inverse kinetics method. Results of the measurements are presented in reference 8. A proton recoil spectrometer has been inserted into the central region of the core for neutron energy spectrum measurements.

The fuel element has been designed so that materials of interest can be added to the core uniformly and cumulatively. Figure 9 shows the critical assembly fuel element design. Note that the axial end reflectors and honeycomb tubes are integral parts of the fuel element. Oralloy rods (93.2 percent uranium 235) are used as the fuel. Three rod sizes were available to allow small adjustments to the fuel loading; the large rods are 0.432-centimeter diameter, the intermediate size is 0.168-centimeter diameter and the small rods are 0.066 centimeter diameter. All are 37.51 centimeters long. Lithium nitride (fully

enriched in lithium-7) is used to simulate both the nitrogen from the UN and coolant of the reference reactor. The ceramic-like lithium nitride pieces fit between the honeycomb tube (Ta) and the fuel tube (Ta). There is sufficient space between the fuel rod bundle and the fuel tube to wrap as much as 4.1 kilograms of hafnium, 15.2 kilograms of tungsten and 21.7 kilograms of tantalum foil distributed uniformly among the 247 fuel elements. In addition, since the full complement of available fuel rods is not needed for criticality, space for an additional 0.279 centimeter diameter tantalum rod is available at the center position of each fuel element. Furthermore, a 0.356 centimeter diameter tantalum rod that is the full length of the fuel element (59.7 cm) can be inserted in the triflute regions between adjacent fuel elements (300 positions) in the star-shaped core region. Parts of these rods extend into the end reflector regions.

Note in figure 9 that there is an eccentricity built into the fuel element. The fuel rod bundle is offset from the center of the honeycomb tube by 0.051 centimeters. This allows simulation of core fuel expansion or compression radially by merely rotating all of the fuel elements. The normal null position is indicated by a fiducial mark on the fuel element end cap that is positioned perpendicular to the radius of the core.

Analysis and Results

The analytical methods used to calculate the critical experiments are very similar to those discussed for the design of the reference reactor. Use of the same methods was convenient to provide precritical calculations of the expected critical masses and desirable to test the validity of these methods. The critical mass predictions, calculated spectra and radial power distributions for a fuel zoned experiment and details of the calculational models are given in references 9, 10, and 11.

Measured and calculated excess reactivities. - The first critical assembly contained 179.64 kilograms of Oralloy. No other materials except those structurally necessary, such as the honeycomb and fuel tubes, were present. The predicted critical mass of 179.7 kilograms (ref. 9) was in remarkable agreement. A relatively large correction of $-0.036 \Delta k$ was applied to the calculated multiplication factor obtained with the S_4P_0 4-group XY TDSN calculation. This correction included $-0.013 \Delta k$ for the difference between lower order and higher order calculations (S_8P_1 13-group), $+0.006 \Delta k$ for structure and materials in the critical assembly that were not conveniently included in the XY calculations, and $-0.029 \Delta k$ for cross section uncertainties estimated from corresponding calculations of several small critical assemblies containing similar materials (see ref. 9 and 12). It is hoped that much of this large discrepancy may be removed by recalculation using ENDF/B cross sections.

Table 2 gives the results of additional experiments and shows a comparison of the measured and calculated excess reactivity in each assembly. Assemblies 1-4 in table 2 have the same uniform fuel loading, amount of hafnium foil and lithium 7 nitride inserts. Materials are added cumulatively to assembly 1 to create assemblies 2-4. The measured and calculated excess reactivity for each assembly is given in the last two columns. Although differences of less than 25 cents are observed between measured and calculated excess reactivities for each assembly, the measured and calculated worth of the incremental material additions have large discrepancies. For example, the measured worth of the tantalum addition in assembly 2 is -50 cents while the calculated worth of this addition is -14 cents. For assemblies 2 and 3 where additional tantalum is added to the core and to the end reflectors the incremental reactivities show less discrepancy. Finally, comparing assemblies 3 and 4, a reactivity of +46 cents was measured for the tungsten addition while the calculation indicates a reactivity of +22 cents. These comparisons indicate that there are errors in the multigroup cross sections of tantalum and tungsten used in the present calculations.

Assembly 5 is a fuel zoned configuration having very closely the same total fuel loading as the previous assemblies (within 30 grams out of about 175 kilograms). Again the measured and predicted total excess reactivity are in very good agreement which indicates the multi-group calculational model used adequately accounts for the reactivity effects of fuel redistribution. A correction of +6 cents has been made to the calculated value of reactivity for this assembly to account for a 120 gram difference in fuel loading between the critical experiment and calculation. The worth of a uniform addition of fuel in these experiments is about 50 cents per kilogram.

It should be reiterated that the same relatively large correction to the calculated 4 group multiplication factor of -0.030 Δk was applied to all five assemblies in table 2. The only difference in the magnitude of this correction term, as used for the first critical experiment described earlier, is that the calculated lower order-to-higher order discrete ordinate approximation effect is -0.007 Δk instead of -0.013 Δk (ref. 11).

Radial power distribution. - Measurements of the radial power distribution for the fuel zoned reactor (assembly 5, table 2) were made at the axial center of the reactor by gamma-scanning the small diameter fuel rods. S_4P_0 4-group calculations (ref. 11) were made prior to the measurements. Figure 10 shows the comparison for each fuel pin in a 30° sector of the reactor. The measurement and calculation agree to within ± 5 percent for all 27 pins measured except one in which the maximum difference is 7 percent. The calculated values of P_r/\bar{P}_r and the measured values are normalized at the second pin from the center. The center pin would ordinarily have been used for this normalization, but the experiment shows an irregular decrease at the center position that cast doubt on the measurements for this particular pin.

Drum control reactivity. - Measurements were made of the reactivity worth of control drums in several of the experimental configurations. The results for a configuration containing all materials except the 0.356-centimeter diameter tantalum rods is shown in figure 11. The inverse counting method ($1/M$) was used (ref. 8) for all 6 control drums ganged which gave 13.45\$ for the total control swing. Estimated accuracy is ± 10 percent. Two detectors, one at the side of the reactor and one at the bottom, were used to obtain the experimental points on figure 11. The dashed curve on figure 11 is an empirical curve ($\sin^2 \theta/2$) found to fit the experimental points rather well. The empirical function has been found to agree with detailed transport calculations of the drum worth also.

The inverse kinetics method (ref. 8) was used to obtain the worth for one drum as 2.15\$. However, this method was found unreliable for measuring large reactivities, such as for all six drums gang-operated, probably because of the slow drum drive-out rate. If there is no significant mutual interaction between adjacent drums, the worth of one drum times six should represent the total control swing. This value ($2.15\$ \times 6$) is 12.90\$. A DOT-IIW S₄P₀ 4-group calculation gave 12.83\$ suggesting that there is no interaction between drums. On the other hand, drum worth experiments for the fuel zoned reactor in which successively 1, 2, 5, and 6 control drums were driven to fuel full-out positions in separate measurements, indicate a drum interaction effect of about 50 cents (0.34 percent $\Delta k/k$) when comparing movement of two opposite versus two adjacent drums. This is smaller than the 0.54 percent $\Delta k/k$ calculated for this effect for the reference reactor.

Neutron energy spectra. - The proton recoil gas proportional counter method was used to measure neutron energy spectra in three of the experimental configurations. The detector was placed at the center of the core. A GAM-II calculation was performed for each case to compare with the experiment. Figure 12 shows the spectrum for the first critical assembly before any additional materials were added. Figure 13 shows the spectrum after 10.1 kilograms of lithium 7 nitride was added. Note the pronounced dip in the flux at about 0.25 MeV caused by the lithium 7 scattering resonance at that energy. Figure 14 shows the spectrum after all materials were added to the core. The lithium 7 resonance effect is still pronounced and well delineated by the experiment. Agreement between the calculation and experiment is qualitatively good for this case except for energy region below ~ 0.08 MeV.

Additional measurements. - The Rossi-alpha technique was used to measure the ratio of the prompt neutron lifetime to the effective delayed neutron fraction, $\lambda/\beta_{\text{eff}}$, for the unzoned configuration containing all the material additions. With $\beta_{\text{eff}} = 0.0067$, an λ of 32 nanoseconds was obtained. This compares with about 40 nanoseconds calculated for the reference reactor and 41 for a configuration very similar to the experiment calculated by Atomics International for the hazards analysis (also reported in ref. 8).

The fuel rotation experiment for the same reactor configuration gave an average value of -47 cents per millimeter for core radial expansion. A calculation for a reactor very similar to the reference reactor gave -39.4 cents per millimeter.

ALTERNATE DESIGNS

Several alternate reactor designs have been considered in this technology program. Figure 15 shows a composite of various designs in cross section. All six designs shown on the figure have the following in common:

1. fuel pin in honeycomb tube design
2. T-111 cladding and pressure vessel
3. TZM end reflectors
4. Lithium 7 coolant; except sodium is used for design D which uses uranium dioxide fuel
5. about two thermal megawatts power level with coolant outlet temperature of 1222 K; except design E which is rated at 0.45 megawatts
6. the benefit of radial power tailoring, not indicated on the figure

The reference reactor is shown in sector A. The sector B reactor is a poison drum controlled reactor using dry wells for the drums which are cooled by radiation to the dry well walls of each drum. Reference 13 discusses a conventional poison drum concept in which the drums are outside of the core pressure vessel. Both uranium 235 and uranium 233 nitride were considered for the fuel. The sector C reactor is controlled by 12 poison rods operating in dry wells and cooled by radiation. Both designs B and C using poison control could have vents for the helium, produced by the $^{10}\text{B}(\text{n},\alpha)^7\text{Li}$ reaction. But behavior of the boron carbide for the long life at high temperatures (of the order of 1600 K) is largely unknown.

The sector D reactor shows a UO_2 design (ref. 14). The benefit in reactor size reduction by using UN is quite apparent upon comparing this reactor with the reference reactor in sector A. Design E is a near minimum size reactor, capable of 0.45 thermal megawatts for 5 years, using uranium 233 nitride. Plutonium 239 nitride would serve about as well as fuel for this reactor. Tantalum beryllide ($\text{Ta}_2\text{Be}_{17}$) was considered for the radial reflector and appears neutronically acceptable. With a density of about 1/2 that of TZM, a considerable reduction in reactor mass is possible; the sector E reactor would weigh about

320 kilograms compared to about 1600 kilograms for the reference reactor. Sector F shows a reactor controlled by axially translating radial reflectors outside the pressure vessel. The sliding reflector pieces are cooled by radiation to the pressure vessel and to a stationary reflector around the reactor (ref. 15). Beryllium oxide canned in molybdenum was also considered for the sliding reflectors of this reactor. However, the combination of molybdenum in the reflector and the pressure vessel (both fairly absorptive of thermal and epithermal neutrons) detracts from the reflector worth so that the beryllium oxide design was no better than the molybdenum design (ref. 16).

Figure 16 shows a side view of the sliding reflector reactor. A major concern for this concept is a water immersion accident. Requiring a movable poison annulus just outside the pressure vessel would detract from the reactivity control and complicate the actuator design.

CONCLUDING REMARKS

A summary of the neutronic results of a technology program using nuclear reactors for the generation of electric power in space has been presented. The discussion was devoted primarily to a reference reactor concept and critical experiments performed to check neutronic calculations. Experiments and calculations are in general agreement. For example, the excess reactivity of several experiments were predicted to within about 25 cents, radial power distributions agreed to within about ± 5 percent, control drum worth also agreed within a few percent and neutron energy spectra comparisons were in reasonable agreement.

However, a persistent discrepancy of about 3 percent in the calculation of absolute multiplication factors ($S_4 P_0$ 4-group) indicates significant errors in some of the neutron cross sections and/or the calculation procedure.

Several alternate reactor design concepts, using different reactivity control methods and materials, were also discussed.

REFERENCES

1. M. H. KRASNER, H. W. DAVISON, and A. J. DIAGUILA: "Conceptual Design of a Compact Fast Reactor for Space Power," to be presented at the Am. Nucl. Soc. 17th Annual Meeting, Boston, Mass. (June 13-17, 1971).
2. R. E. GLUYAS and A. F. LEITZKE: "Material Technology Program for the Compact Fast Reactor for Space Power," to be presented at the Am. Nucl. Soc. 17th Annual Meeting, Boston, Mass. (June 13-17, 1971).

3. C. L. WHITMARSH, Jr., "Neutronic Design for a Lithium-Cooled Reactor for Space Applications," TN D-6169, NASA (1971).
4. G. D. JOANOU, and J. S. DUDEK, "GAM-II. A B3 Code for the Calculation of Fast-Neutron Spectra and Associated Multigroup Constants," GA-4265, General Atomics Div., General Dynamics Corp. (Sept. 16, 1963).
5. C. E. BARBER, "A FORTRAN IV Two-Dimensional Discrete Angular Segmentation Transport Program," TN D-3573, NASA (1966).
6. R. G. SOLTEZ, R. K. DISNEY, and G. COLLIER, "Users Manual for the DOT-IIW Discrete Ordinates Transport Computer Code," WANL-TME-1982, Westinghouse Astronuclear Lab., Westinghouse Electric Corp. (December 1969).
7. G. D. JOANOU, C. V. SMITH, and H. A. VIEWEG, "GATHER-II, An IBM-7090 FORTRAN-II Program for the Computation of Thermal-Neutron Spectra and Associated Multigroup Cross-Sections," GA-4132, General Dynamics Corp. (July 8, 1963).
8. W. H. HENEVELD, et al., "Experimental Physics Characteristics of a Heavy Metal Reflected Fast Spectrum Critical Assembly," NASA CR-72820, Atomics International (1971).
9. W. MAYO, and E. LANTZ, "Analysis of Fuel Loading Requirements and Neutron Energy Spectrum of a Fast-Spectrum, Molybdenum-Reflected, Critical Assembly," TM X-52762, NASA (1970).
10. J. L. ANDERSON and W. MAYO, "Effect of Adding Lithium Nitride, Hafnium, Tantalum, and Tungsten to a Fast-Spectrum Molybdenum-Reflected Critical Assembly," TM X-52787, NASA (1970).
11. W. MAYO, "Precritical Analysis of a Power-Tailored Fast-Spectrum Molybdenum-Reflected Critical Assembly," TM X-52895, NASA (1970).
12. P. G. KIANN, W. MAYO, and T. H. SPRINGER, Trans. Am. Nucl. Soc., 13, 731 (1970).
13. W. MAYO, and R. M. WESTFALL, "Reflector-Based Poison-Drum Control on Equal-Size Reactor Cores Fueled with Uranium-233 and with Uranium-235, TM X-1883, NASA (1969).
14. W. MAYO, and R. M. WESTFALL, "Radial Power Tailoring for a Uranium Dioxide - T-111 Clad Reactor with Contained Fission Product Gases," TM X-1795, NASA (1969).
15. W. MAYO, C. L. WHITMARSH, Jr., J. V. MILLER, and H. W. ALLEN, "Characteristics of a 2.17-Megawatt Fast-Spectrum Reactor Concept Using an Axially Moving Reflector Control System," TM X-1911, NASA (1969).

16. C. L. WHITMARSH, Jr. and W. MAYO, "Neutronic Comparison of Beryllium Oxide and Molybdenum for Movable Reflector Control of a Fast-Spectrum Reactor," TM X-1822, NASA (1969).

TABLE 1. - REACTIVITY COMPONENTS OF CONTROL SWING

Component	Reactivity, percent $\Delta k/k$
Fuel burnup	1.47
Temperature defect:	1.09
Coolant expansion (0.26)	
Fuel and structure expansion (0.58)	
Doppler (0.25)	
Fuel swelling	.95
Uncertainty allowance	<u>.61</u>
Total excess reactivity	4.12
Shutdown margin	<u>4.39</u>
Total control swing	8.51

TABLE 2. - REACTIVITY COMPARISONS

Assembly	Core materials	Reactivity, ϵ		
		Measured NASA CR-72820	Predicted NASA TM X-52895	
1	Base (175 Kg U, 4 Kg H _f , 10 Kg ⁷ Li ₃ N)	175	175	158
2	Base + 22 Kg Ta foil + 10 Kg Ta rods (0.279 cm)	125		144
3	Assembly 2 + 19 Kg Ta rods (0.356 cm) (+11 Kg in end reflectors)	80		104
4	Assembly 3 + 15 Kg W	126		126
5	Assembly 4 but fuel zoned, no Ta rods	38		^a 29

^a $\Delta +6\epsilon$ correction for fuel difference included.

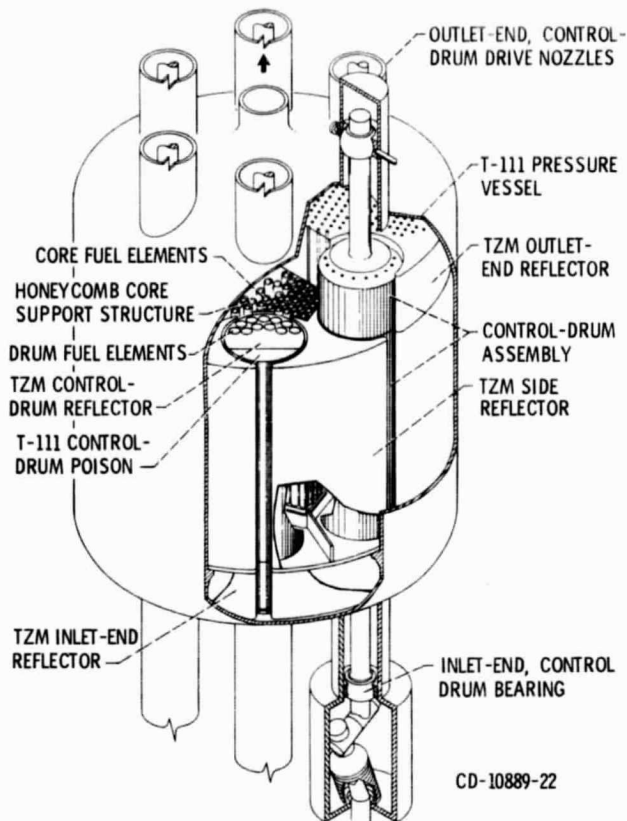


Figure 1. - Space power reference reactor.

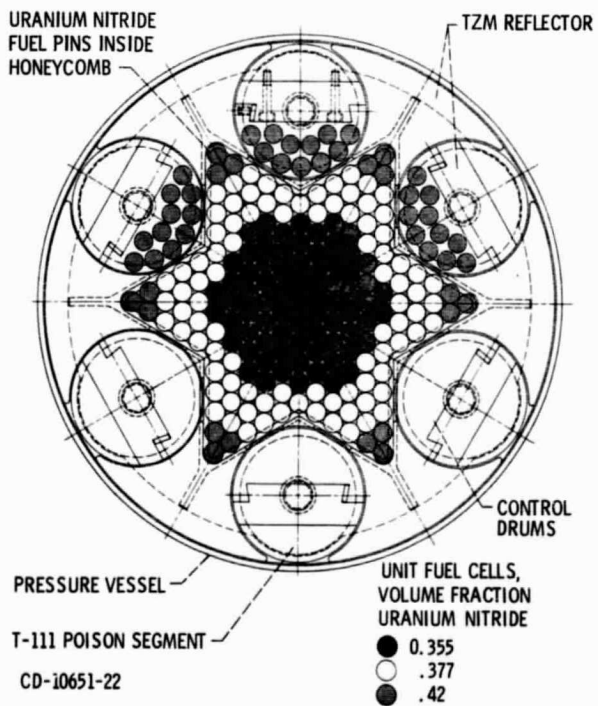


Figure 2. - Cross section of reference reactor.

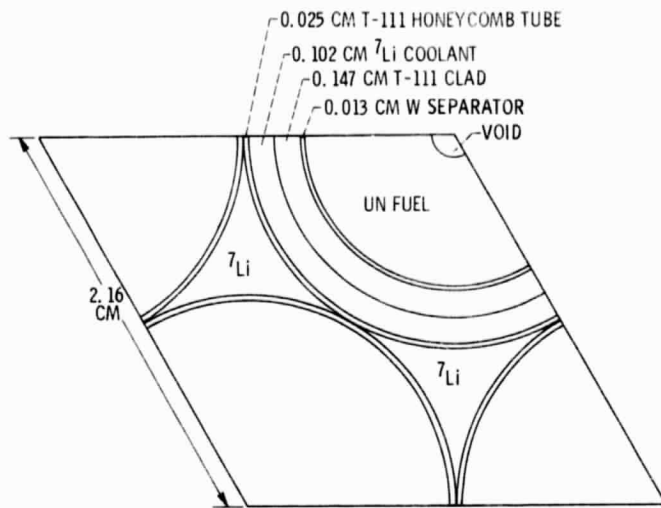


Figure 3. - Cell and fuel pin geometry.

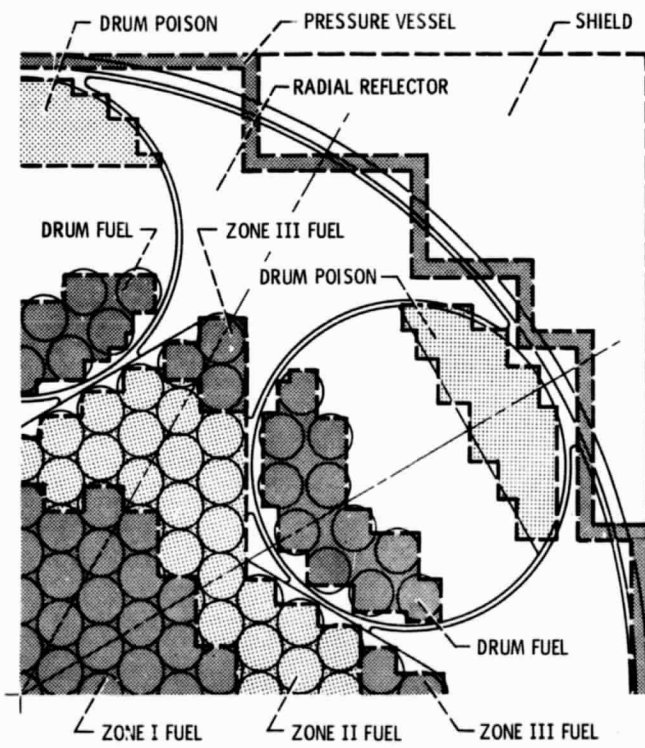


Figure 4. - XY calculation model.

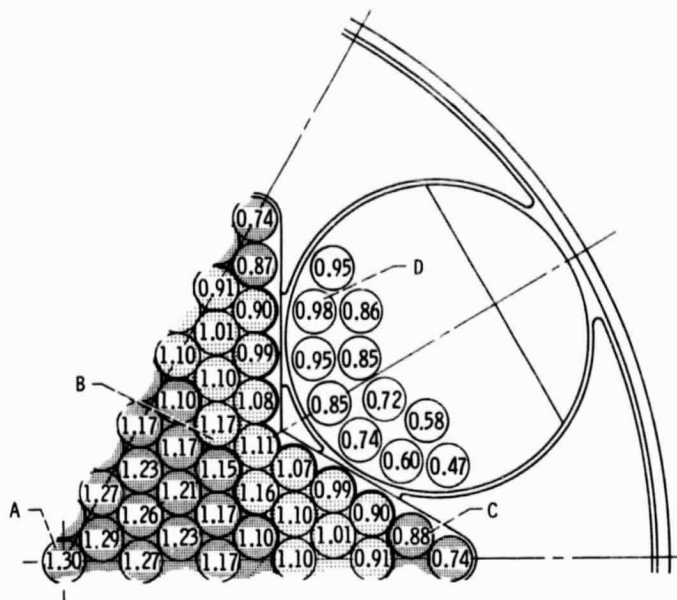


Figure 5. - Radial power ratios averaged over 50 000 effective full-power hours of reactor operation.

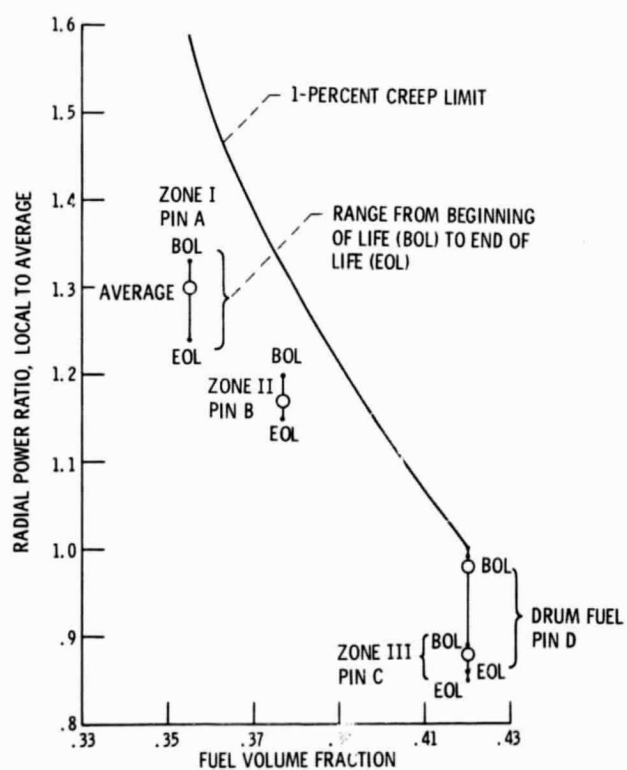


Figure 6. - Calculated radial powers of the peak pin in each fuel zone compared to the creep limited power. Average burnup, 2.44 percent total uranium; average fuel fraction, 0.385; axial peak-to-average power, 1.23.

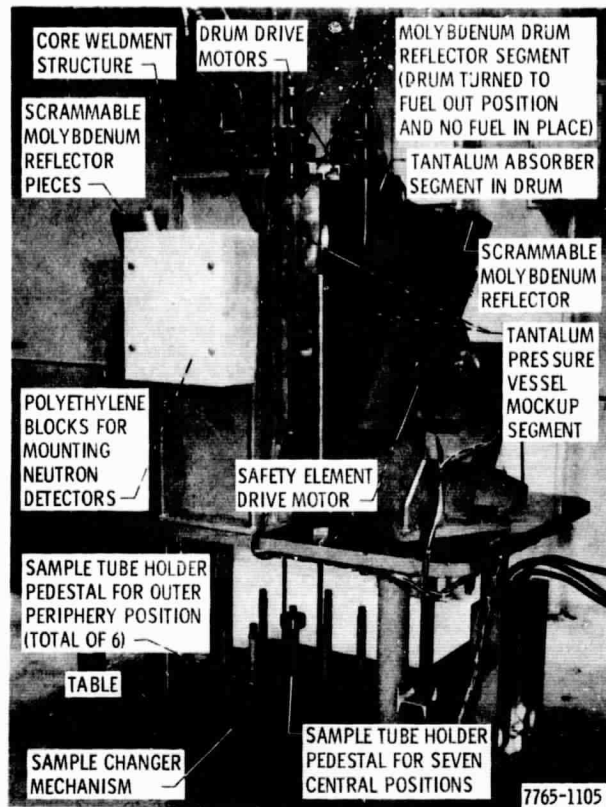


Figure 7. - Critical assembly.

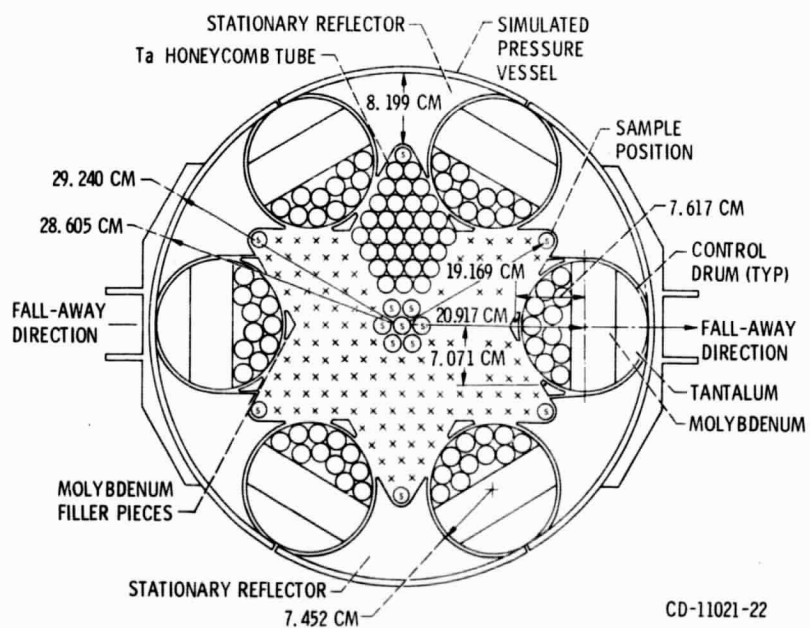


Figure 8. - Cross section of critical assembly.

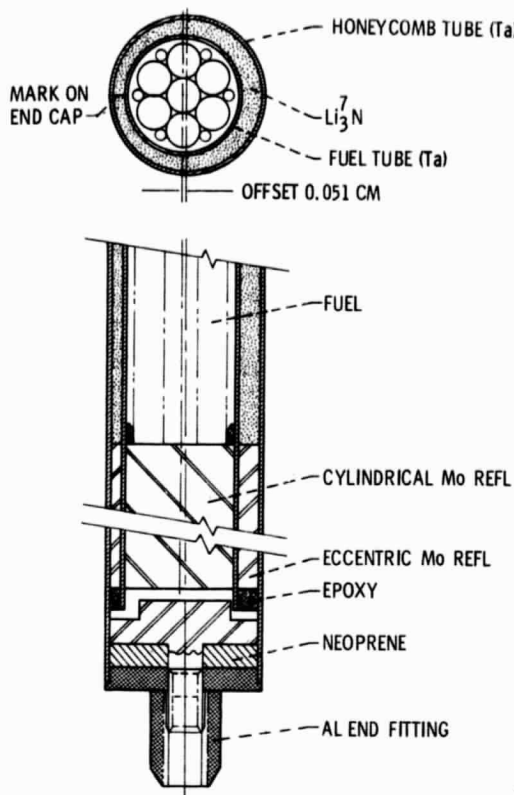


Figure 9. - Fuel element for critical experiments.

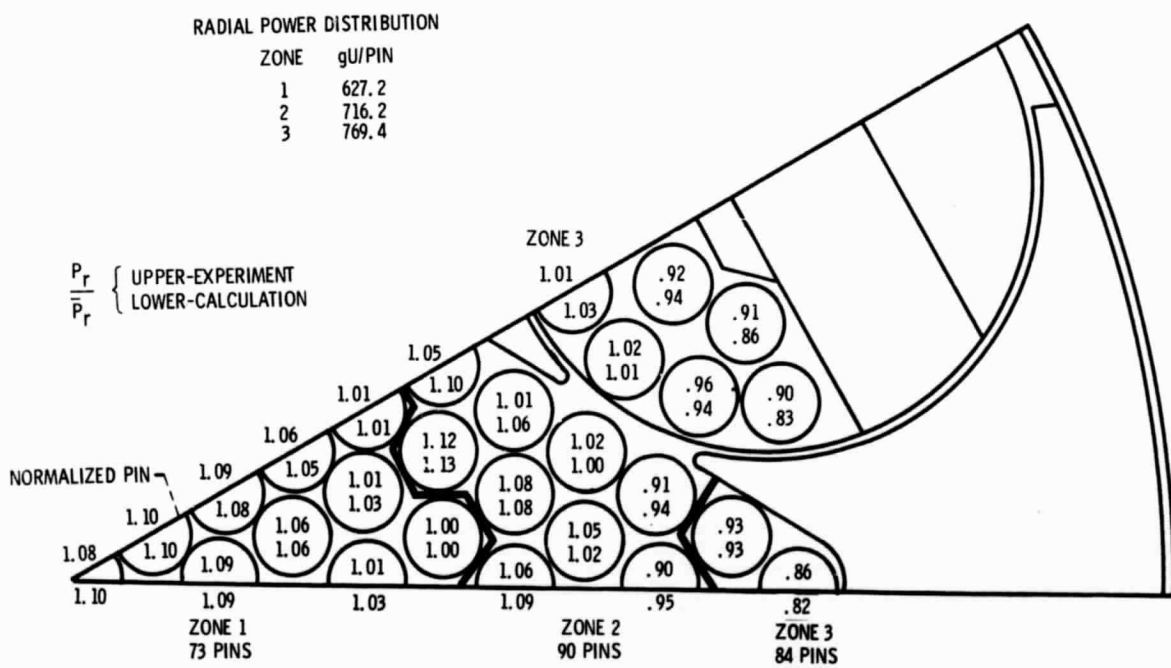


Figure 10. - Measured and calculated radial power distribution for fuel zoned reactor.

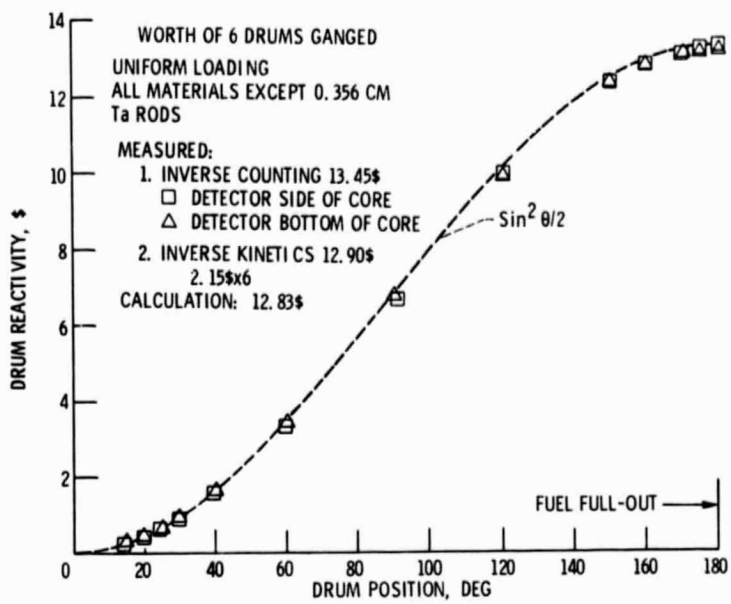


Figure 11. - Measured and calculated control drum reactivity.

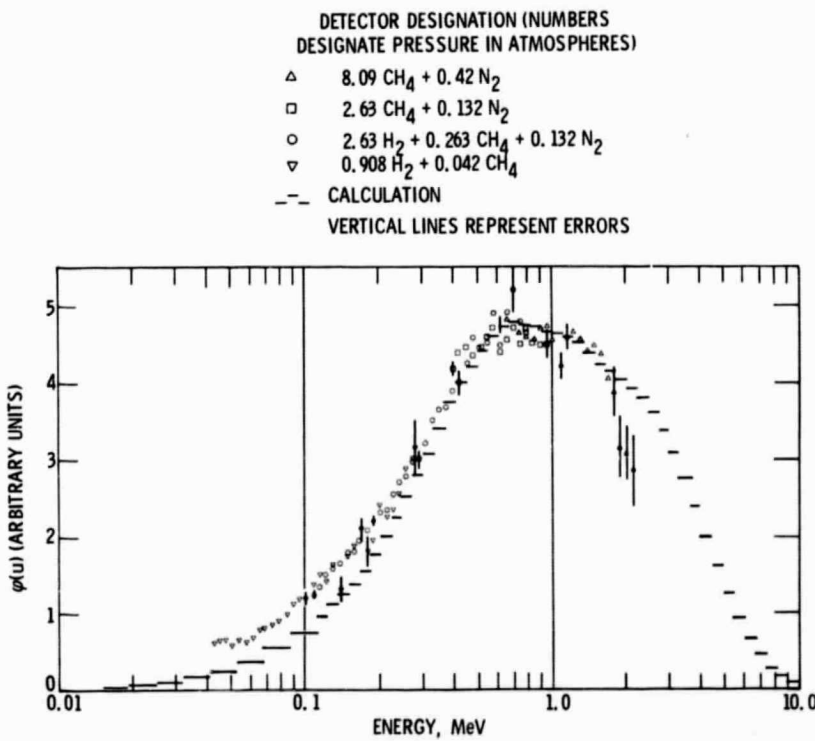


Figure 12. - Spectrum for experiment containing only Oralloy fuel.

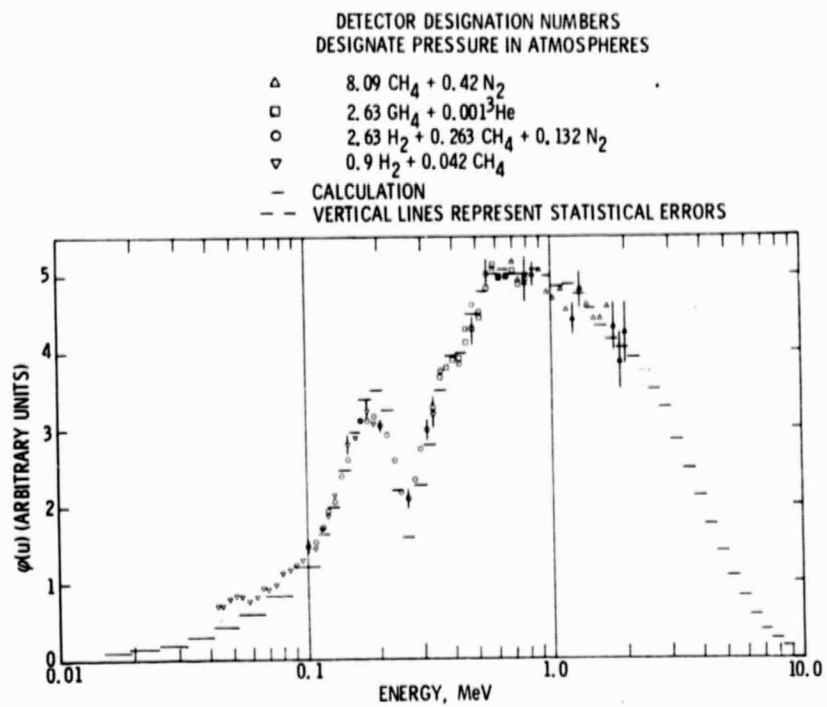


Figure 13. - Spectrum with 10.1 kilograms of lithium nitride added to core.

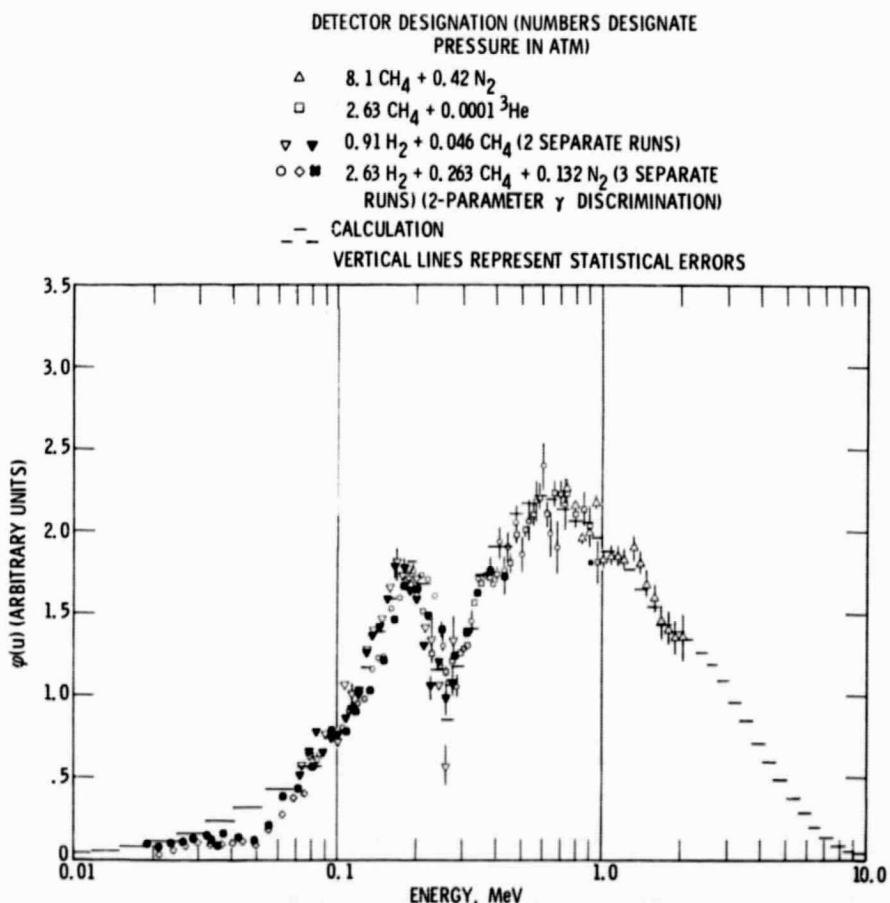


Figure 14. - Spectrum with all materials in core (uniform loading).

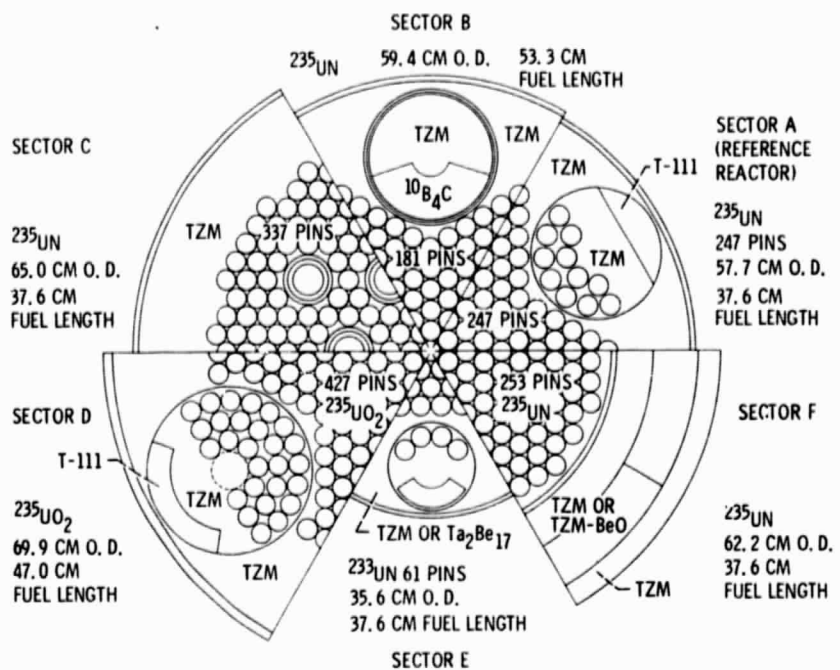


Figure 15. - Alternate reactor concepts compared with reference reactor.

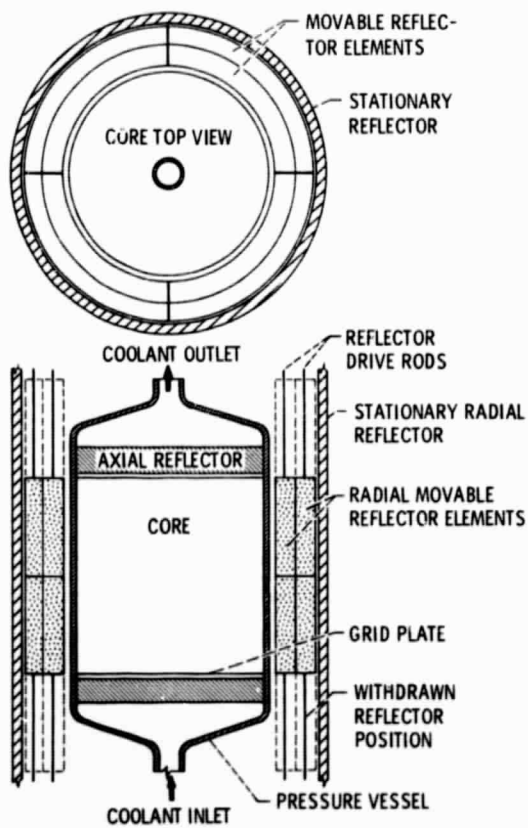


Figure 16. - Side view of reactor controlled by sliding reflectors.